RADIATION RESEARCH **185**, 000–000 (2016)
0033-7587/16 $15.00

DOI: 10.1667/RR14226.1

Differential Response and Priming Dose Effect on the Proteome of Human Fibroblast and Stem Cells Induced by Exposure to Low Doses of Ionizing Radiation

Monika Hauptmann,[a,1] Siamak Haghdoost,[c] Maria Gomolka,[a] Hakan Sarioglu,[b] Marius Ueffing,[b] Anne Dietz,[a] Ulrike Kulka,[a] Kristian Unger,[d] Gabriele Babini,[e] Mats Harms-Ringdahl,[c] Andrea Ottolenghi[e] and Sabine Hornhardt[a]

[a] *Federal Office for Radiation Protection, Department SG Radiation Protection and Health, Oberschleissheim, Germany;* [b] *Helmholtz Zentrum München, German Research Center for Environmental Health, Department of Protein Science, Neuherberg, Germany;* [c] *Center for Radiation Protection Research, Department of Molecular Biosciences, The Wenner-Gren Institute, Stockholm University, Stockholm, Sweden;* [d] *Helmholtz Zentrum München, German Research Center for Environmental Health, Department of Radiation Cytogenetics, Neuherberg, Germany; and* [e] *Department of Physics, University of Pavia, Pavia, Italy*

Hauptmann, M., Haghdoost, S., Gomolka, M., Sarioglu, H., Ueffing, M., Dietz, A., Kulka, U., Unger, K., Babini, G., Harms-Ringdahl, M., Ottolenghi, A. and Hornhardt, S. Differential Response and Priming Dose Effect on the Proteome of Human Fibroblast and Stem Cells Induced by Exposure to Low Doses of Ionizing Radiation. *Radiat. Res.* 185, 000–000 (2016).

It has been suggested that a mechanistic understanding of the cellular responses to low dose and dose rate may be valuable in reducing some of the uncertainties involved in current risk estimates for cancer- and non-cancer-related radiation effects that are inherited in the linear no-threshold hypothesis. In this study, the effects of low-dose radiation on the proteome in both human fibroblasts and stem cells were investigated. Particular emphasis was placed on examining: 1. the dose-response relationships for the differential expression of proteins in the low-dose range (40–140 mGy) of low-linear energy transfer (LET) radiation; and 2. the effect on differential expression of proteins of a priming dose given prior to a challenge dose (adaptive response effects). These studies were performed on cultured human fibroblasts (VH10) and human adipose-derived stem cells (ADSC). The results from the VH10 cell experiments demonstrated that low-doses of low-LET radiation induced unique patterns of differentially expressed proteins for each dose investigated. In addition, a low priming radiation dose significantly changed the protein expression induced by the subsequent challenge exposure. In the ADSC the number of differentially expressed proteins was markedly less compared to VH10 cells, indicating that ADSC differ in their intrinsic response to low doses of radiation. The proteomic results are further discussed in terms of possible pathways influenced by low-dose irradiation.

INTRODUCTION

The average population is constantly exposed to low doses of ionizing radiation (2–4 mSv/year) from both environmental and man-made sources, and to date, the possible health effects from these exposures have not been verified. However, current risk models indicate that exposure to a 2 mSv dose could cause more than 70,000 cancer cases per year in Europe. This risk estimate is based on the linear no-threshold hypothesis, as applied in the international rules and standards in radiation protection (*1*).

The scarcity of scientifically based risk estimates for cancer and non-cancer-related effects from exposure to low-dose radiation presents a challenge for the scientific community, since these estimates are necessary to address the lack of sensitivity in epidemiological methods for doses $<$50 mSv (*2*). Thus, new strategies are needed to gain a deeper understanding of the health risks associated with exposure to low doses of radiation. Recent advances in biotechnology demonstrated that the cellular response to doses in the mGy range can be monitored (*3–7*) on gene and protein levels and that a systems biology approach may provide a promising tool for the mechanistic understanding of low-dose effects on cells and organs.

Emerging evidence indicates that the transcriptional and translational responses to doses in the range of 1–100 mGy may differ significantly (*8–11*), as well as for altered protein posttranslational modifications (*12*). The findings that cancer risks from low-dose exposure may be under- or overestimated due to radiation-induced bystander effects (*13*) and adaptive responses (*14, 15*) underlines the

Editor's note. The online version of this article (DOI: 10.1667/RR14226.1) contains supplementary information that is available to all authorized users.

[1] Address for correspondence: Federal Office for Radiation Protection, Department SG Radiation Protection and Health, Ingolstädter Landstraße 1, 85764 Oberschleissheim, Germany; email: mhauptmann@bfs.de.

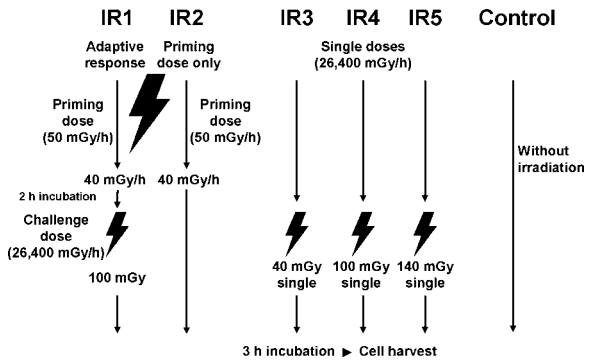

FIG. 1. Experimental design. Exposure conditions for VH10 cells (IR1–IR5). The ADSC were exposed only to conditions IR1, IR4 and IR5.

importance of a mechanistic understanding of the low-dose and dose-rate effects. Thus, the effect of low doses at the level of gene and protein expression is unpredictable from the changes induced by high doses with possible consequences for a phase shift in the current view of linear dose-response relationships.

In a radiation-induced adaptive response, first reported by Olivieri *et al.* (*16*), the induced damage in cells exposed to a priming dose (usually within the dose range of 1–100 mGy), briefly followed by a challenge dose, is less than the induced damage from the challenge dose given alone. Thus, a priming exposure can protect against subsequent damage induced by a second exposure. In addition, it has been reported that a relatively narrow window of priming doses was observed to be effective when delivered at an appropriate dose rate and depending on the total dose applied (*17*). This means that the cells must receive a certain amount of detriments within a given interval of time for the adaptive response to be expressed. It might also be possible that the dose range required to induce the adaptive response depends on the cell sensitivity or might be restricted to specific experimental systems or biological end points rather than a general phenomenon. It is not yet clear if and how an adaptive response has the potential to affect the dose response at low doses of radiation. Novel research results even suggest a relationship between bystander effect and adaptive response because the bystander effect may play a crucial role in the induction of the adaptive response concerning low-dose irradiation (*18*).

The controversy over risk estimates for low doses also includes the dose-rate effect. This is illustrated in the debate over the scientific support for the dose and dose-rate effectiveness factor (DDREF) of 2 (*19*). It was shown that for suppression of neoplastic transformation the adaptive response was dose-rate dependent (*20*) and that the so-called inverse dose-rate effect shown by enhanced mutations at very low-dose rates (*21, 22*) needs to be taken into consideration. However, in a recent work where TK6 cells were exposed at low-dose rates of 1.4–30 mGy/h, there was no indication of a dose-rate effect on the yield of mutations in the thymidine kinase locus (*23*).

To elucidate the molecular mechanisms in dose-response relationships as they relate to low-dose effects we analyzed cellular response in terms of radiation-induced changes in a protein expression profile combined with pathway analysis. For this purpose, we: 1. explored how the profile of the normal human skin fibroblast and stem cell proteome respond to low doses (40–140 mGy) delivered at a dose rate of 26,400 mGy/h; 2. investigated how a priming dose of 40 mGy changes the protein expression profile of a challenge dose; and 3. applied pathway and network analysis on the differentially regulated proteins. Based on the differential protein expression at different exposure conditions, changes in pathways were identified, which differentiated between doses and dose rates as well as the effect of a priming dose. Marked differences in radiation-induced protein expression between differentiated VH10 cells and stem cells were also observed.

MATERIALS AND METHODS

Cell Culture

Primary human fibroblast cells used in this study were from normal human diploid foreskin fibroblast cell strain VH10 (from Leiden University, The Netherlands). All experiments were performed with passage 11. Six-cell culture flasks (175 cm^2) were prepared according to the experimental set-up. Each experiment was repeated independently three times. One-million (10^6) cells were cultured in Dulbecco's modified Eagle medium (DMEM) (Invitrogen, Paisley, UK) containing 10% defined bovine serum (GE Healthcare Life Sciences/ HyClone™ Laboratories, Logan, UT) and protein-tyrosine phosphatase (Invitrogen). The cells were grown in each flask for 3 weeks at 37°C in 5% CO_2 until confluence. Cell culture media was changed every 5 days.

StemPro® human adipose-derived stem cells (ADSC) were obtained from Invitrogen™ (Carlsbad, CA). These cells are isolated from human adipose tissue collected during liposuction procedures and cryopreserved from primary cultures. Before cryopreservation, the ADSC are expanded for one passage in MesenPRO RS™ medium. Each lot of ADSC originates from a single donor of human lipoaspirate tissue. The cells were cultured in MesenPRO RS basal medium and MesenPRO growth supplement provided as a kit by Invitrogen. Each experiment was independently repeated 4 times. The cells were handled in the same manner as the primary human fibroblast cells. For sub-culturing Accutase™ was used. Cells were cultured in 175 cm^2 flasks until confluence (12 days) and media was changed every fourth day.

Irradiation Conditions

For irradiation of the cells two different ^{137}Cs sources were used. For acute exposure a ^{137}Cs source (Scanditronix, Uppsala, Sweden) with a dose rate of 26,400 mGy/h was used. A cell culture incubator (37°C) equipped with a custom-made ^{137}Cs source was used to expose the cells to 40 mGy at the dose rate of 50 mGy/h. Irradiation conditions (IR1–IR5) are summarized in Fig. 1. Under condition IR1 the cells were exposed to 40 mGy priming dose (50 mGy/h) followed by a challenge dose of 100 mGy, delivered at 26,400 mGy/h after 2 h incubation. This was done to investigate possible adaptive response effects when compared to condition IR4, where only the challenge dose was delivered. The second irradiation condition (IR2) consisted only of the priming dose of 40 mGy (50 mGy/h). Conditions IR3, IR4 and IR5 included an increasing challenge dose (40, 100 and 140 mGy delivered at 26,400 mGy/h) to study the dose-response relationship of

the proteome in the low-dose range. Sham-irradiated cells were used as control.

Cells were harvested 3 h postirradiation after high-dose-rate exposures. This was determined as the optimal time point with the largest amount of differentially regulated proteins in a time kinetic experiment (cell harvest 0.5, 3 and 24 h postirradiation) done prior to this work (data not shown). Cells were washed 3 times with Hanks' balanced salt solution (HBSS) without calcium and magnesium. To detach the cells, 2 ml trypsin-EDTA (Invitrogen) was added to each flask and incubated for 7 min at 37°C. The cells were collected in a tube by centrifugation (10 min, 250*g*) and washed 3 times with HBSS. The weight of each cell pellet was determined. The cell pellets were kept at −25°C for one week and then sent from Stockholm University to the Federal Office for Radiation Protection (Oberschleissheim, Germany) under frozen conditions for proteome analysis.

Two-Dimensional Difference in Gel Analysis (2D-DIGE)

Frozen cells were put on ice for 5 min, gently lysed (7 *M* urea, 2 *M* thiourea, 25 m*M* Tris, 4% CHAPS and 10 µl/mg cell pellet), sonicated and centrifuged (30 min, 22,000*g*, 4°C).

The protein concentration of the supernatants was determined in duplicate by the *RC DC*™ g as recommended by the manufacturer (Bio-Rad Laboratories Inc., Hercules, CA) using bovine serum albumin (BSA) as standard.

The chosen proteomic strategy was based on two-dimensional (2D) gel electrophoresis enhanced by the use of the 2D-DIGE (*24, 25*). The experimental set-up consisted of one control and five different exposure conditions (IR1–IR5) each comprised of three (VH10 cells) or four (ADSC) individual biological replicates harvested at one time point after exposure (3 h).

Three samples (total of 150 µg, 50 µg each) were each dissolved in 30 µl lysis buffer and labeled with Cy2 (IS), Cy3 and Cy5 (CyDye™ DIGE Fluor minimal dyes; GE Healthcare, Munich, Germany) according to the manufacturer's instructions. To eliminate dye-specific differences, one aliquot of each fibroblast sample was labeled with Cy3 and a second with Cy5 (inverse labeling or dye swap) leading to two independent gels from each sample (DIGE 1 and DIGE 2). No dye swap was performed using the stem cells. An internal standard (IS) was pooled of equal protein amounts of all replicates (nonirradiated, IR1–IR5) and labeled with Cy2. Labeled samples consisted of 150 µg and 3 samples, internal standard (IS), sample Cy3 and sample Cy5, were applied on a single gel.

ReadyStrip™ (18 cm long) immobilized pH gradient (IPG) strips, pH 3–10 NL (Bio-Rad), were rehydrated passively overnight [6 *M* urea, 2 *M* thiourea, 100 m*M* dithiothreitol (DTT), 2% CHAPS, 0.5% (v/v) Pharmalyte™ pH 3–10]. The labeled samples were supplemented with 5 µl DTT (40 mg DTT diluted in 75 µl H_2O) and 1 µl Pharmalyte pH 3–10 (GE Healthcare) and then applied onto the rehydrated IPG strips by anodal cup loading. First-dimension isoelectric focusing (IEF) was performed on a PROTEAN® IEF Cell device (Bio-Rad) at 20°C for a total of 33–35 kVh. For the second dimension, the strips were placed on top of a handcast linear SDS-containing 13% polyacrylamide gels using low-fluorescence glass plates of 26 × 20 cm (PROTEAN Plus Dodeca™ Cell 12-gel system; Bio-Rad) and fixed with 0.8% agarose in running buffer (0.1% SDS, 192 m*M* glycine, 0.025% Tris) containing Bromophenol blue. For molecular weight range determination, a molecular weight marker (10–200 kDa; Bio-Rad) was applied with a paper plug along with sodium dodecyl sulfate polyacrylamide gel electrophoresis (SDS-PAGE) separation.

After electrophoresis, gels were scanned directly between glass plates using a Typhoon™ 9400 (GE Healthcare) with the appropriate excitation and emission wavelengths for Cy2, Cy3 and Cy5 dyes. Images were cropped in ImageQuant™ software v 5.2 (GE Healthcare).

After image acquisition, the gels were fixed in 30% ethanol and 10% acetic acid for 2 h, kept in 1× Flamingo™ stain (Bio-Rad) overnight and then stained with Coomassie. The gels were stored at 4°C until spot excision for mass spectrometric analysis. Coomassie images were acquired on the GS-800™ imager (Bio-Rad).

Gel Analysis and Statistics

Protein spot abundances and statistics were analyzed by DeCyder™ Image Analysis Software v 7.0 (GE Healthcare). Gel images were grouped for comparison. Each individual group was comprised of the images of three biological replicates leading to 18 compared gels in total (control, IR1–IR5). All gel images were matched automatically and normalized using the internal standard (labeled in Cy2). Significantly changed protein spots were determined by the following procedure: 1. The spot was matched across 16 of 18 gels; and 2. Spots were considered to be differentially regulated if a statistically significant difference in intensity was achieved. To investigate the significantly deregulated proteins for one condition, a two-tailed Student's *t* test was performed ($P \leq 0.05$). The comparison of more than two treatments, when the samples are normally distributed, was performed by one-way analysis of variance (one-way ANOVA). Differences among radiation exposure conditions were analyzed by one-way ANOVA ($P \leq 0.05$) to detect the extent to which observed variances between the different conditions could be explained by the experimental parameters, as opposed to biological or technical variation.

DeCyder™ Extended Data Analysis Software (DeCyder EDA), a high-performance informatics software for the analysis of large and combined proteomics data sets, was used to perform a first statistical approach with the raw data. This tool performs multivariate statistics tailored for 2D gel image data, like principal component analysis (PCA) and hierarchical clustering. PCA or the related singular value decomposition was applied to test the data for main factors contributing to the observed effects. PCA, which reduces the dimensionality of a data set by defining principal components that describe a percentage of the total variance of the data, was applied to the gel images.

Mass Spectra (MS) Analysis of Differentially Regulated Proteins and Data Processing

Protein spots were chosen for mass spectrometry if they could be clearly identified as such and removed from gels without contamination from nearby proteins. Spots were manually excised from the gels, destained and washed with buffer containing 50 m*M* NH_4HCO_3 in 30% acetonitrile (ACN) and equilibrated in 10 m*M* NH_4HCO_3 prior to proteolytic digestion. Gel pieces were shrunk with 100% v/v ACN and rehydrated in 10 m*M* NH_4HCO_3. This treatment was repeated, followed by the addition of 0.1–0.2 µg of modified trypsin (Sigma-Aldrich, St. Louis, MO) per piece. Digestion was performed overnight at 37°C. The supernatant was collected and combined with the eluates of subsequent elution steps with 80% v/v ACN, 1% v/v trifluoroacetic acid (TFA). The combined eluates of one gel piece were dried in a SpeedVac™ centrifuge. The dry samples were dissolved in 20 µl 50% v/v ACN, 0.1% v/v TFA for the subsequent MALDI preparation. A 1:1 mixture of sample and a matrix solution (0.5 µl) consisting of 5 mg/ml α-cyano-4-hydroxycinnamic acid (Bruker Daltonik, Bremen, Germany) were manually spotted on a MALDI target.

Mass spectra were acquired using a 4700 Proteomics Analyzer (matrix-assisted laser desorption-ionization/time-of-flight: MALDI-TOF/TOF) mass spectrometer (Applied Biosystems®, Framingham, MA). Measurements were performed with a 355 nm Nb:YAG laser in positive reflector mode with a 20 kV acceleration voltage. For each MS and MS/MS spectrum 3,000 spots were accumulated. For each spot on a MALDI plate the eight most intense peptides were selected for additional MS/MS analysis. The acquired MS/MS spectra were searched with GPS Explorer™ v 3.6 (AB Sciex™, Framingham, MA) against the Ensembl_human database (updated August 2014; 105288 sequences, 40047886 residues) using an in-house version of Mascot 2.3.02 with the following parameters: As taxon we chose human/mammalia and as enzyme trypsin allowing up to one missed cleavage.

TABLE 1
Number of Significantly Altered Protein Spots Detected by Decyder Software Postirradiation

Exposure conditions	Priming dose rate (mGy/h)	Challenge dose rate (mGy/h)	Total dose (mGy)	Total spots (master gel)	Candidate spots (t test, $P \leq 0.05$; raw data)[a]	Confirmed spots
IR1	50	26,400	40 + 100	2,323	114	50
IR2	50	-	40	2,323	115	48
IR3	-	26,400	40	2,323	105	36
IR4	-	26,400	100	2,323	89	28
IR5	-	26,400	140	2,323	42	7

[a] Mean values of three biological replicates.

We set carbamidomethylation as fixed modification and oxidized methionine as variable modification (*26*).

The Mascot protein score reflects the combined scores of the peptide mass fingerprint score for the MS spectra as well as the sum of all ion scores for a successful MS/MS spectrum. A protein was therefore regarded as identified if the following three criteria were fulfilled: 1. The probability-based molecular weight search (MOWSE) score was above the 5% significance threshold for the respective database (95% confidence level) (for the used version of Ensembl_human db a protein score higher than 55); 2. The matched peptide masses were abundant in the spectrum; and 3. The theoretical isoelectric point (pI) and the molecular weight of the search result could be correlated with the 2D position of the corresponding spot. MS/MS spectra of protein identifications with scores near the significance level are always manually checked.

Western Blot

For the validation of protein regulation, the sensitive Stain-Free Western blot technology (Bio-Rad), using total protein quantification for normalization, was applied (*27, 28*). This technology offered a perspective to bypass the fact of deregulated housekeeping proteins after irradiation of cells. The signal of the entire sample loaded in the corresponding lane was used as a loading control for the target protein signal. An in-gel chemistry was activated under ultraviolet excitation and the fluorescing protein quantity was detected by suitable imaging systems either within the gel or after transfer to a blotting membrane.

According to determined protein concentration, 10 or 20 µg total cell extract of each irradiated sample and respective control in Laemmli buffer containing 25 m*M* Tris/HCl pH 7.5, 2% SDS, 15% glycerol and 1% DTT, together with marker proteins (Precision Plus Protein™ Unstained Standards; Bio-Rad) were loaded onto Criterion™ TGX Stain-Free™ Any kD™ gels (Bio-Rad) and separated for 1 h and 30 min (30 min/20 mA and 70 min/40 mA per gel).

Proteins were transferred to nitrocellulose membranes using the Trans-Blot® Turbo™ Transfer System (Bio-Rad) at 2.5 A for 7 min and saturated overnight in Tris-buffered saline (TBS; 50 m*M* Tris-HCl, pH 7.6 and 150 m*M* NaCl) containing 5% BSA. After washing three times in TBS/T (TBS, 0.1% Tween® 20) blots were incubated for 3 h at room temperature with primary antibodies against chosen target proteins, such as the following: chloride intracellular channel protein 1 (CLIC1, cat. no. ab77214, lot GR71847-1, 1:1,000), lamin A (LMNA, cat. no. ab108595, lot GR48714-17, 1:500), superoxide dismutase 2 (SOD2, cat. no. ab16956, lot GR13155-1, 1:10,000), vinculin (VCL, cat. no. ab18058, lot GR53348-1, 1:1,000), eukaryotic elongation factor 2 (EEF2, cat. no. ab33523, lot GR26010-1, 1:500) (supplied by Abcam®) and vimentin (VIM, Calbiochem®; cat. no. IF01, lot D00073488, 1:5,000) diluted in TBS/T containing 5% BSA.

After washing three times in TBS/T, blots were incubated for 1 h at room temperature with alkaline phosphatase (AP)-conjugated [anti-mouse (cat. no. A3562), anti-rabbit (cat. no. A3687); Sigma-Aldrich] or horseradish peroxidase (HRP)-conjugated secondary antibody [anti-mouse (cat. no. 170-5047), anti-rabbit (cat. no. 170-5046); Immun-Star™, Bio-Rad] in blocking buffer (TBS/T, 5% BSA). Protein bands were visualized using the AP and HRP conjugate substrate kits (both from Bio-Rad). After AP-immunodetection the membranes were dried overnight and scanned with a GS-900™ scanner (Bio-Rad). Fluorescent blot images (HRP) were collected immediately using the ChemiDoc™ MP system (Bio-Rad). Protein signals were quantified using Image Lab™ software (v 5.0; Bio-Rad) and normalized to the total protein amount loaded on the corresponding lane. The normalized data sets were used for the calculation of protein regulation levels. In addition, double-sided and paired t tests were performed with Microsoft Excel XP software to evaluate the statistical significance of the calculations.

Pathway Analysis

For pathway analysis, the Reactome FI PlugIn tool was used [Cytoscape, plugin for http://www.cytoscape.org] (*29*). In this approach solely identified proteins with statistically significant regulation changes are addressed and, if relevant, displayed by the software as circles and potential linkers, for example, proteins that are not part of the protein list but that permit indirect interaction between two proteins are indicated by diamond-shaped symbols (both so-called nodes). Interrelations (so-called edges) between these proteins are shown either by a dashed line (predicted), a solid black line (experimental evidence), an arrow-headed line (type of interaction is known) or a bar-headed line (inactivation/suppression). In addition, the discovery of modules (subnetworks) within a network helps isolate systems with radiation-related properties and reduces interactome complexity. To further characterize the modules induced by low-dose irradiation, we looked for significantly enriched biological pathways associated with the different exposure conditions and retrieved the most prominent pathways for each module. Modules with a small number of listed pathways ($\leq$7 pathways), and thus without dominant network features, were not enlisted. Due to the small number of only three significant proteins, IR5 was not investigated further.

RESULTS

Differential Protein Expression Analysis of DIGE gels in VH10 Fibroblast Cells

Raw Data

The number of significantly deregulated spots according to the irradiation conditions (IR1–IR5) are shown in Table 1. This table compares the number of total spots detected under the different irradiation conditions IR1–IR5, as well as the number of candidate spots that were significantly ($P \leq 0.05$) differentially expressed compared to nonirradiated control cells. Subsequently, these spots were evaluated based on the mean value among the sample groups and were manually controlled to identify possible artefacts (e.g., staining and other background artefacts). Only manually confirmed spots were analyzed by mass spectrometry.

Confirmed candidate spots were analyzed by MALDI-TOF/TOF tandem mass spectrometry and peptide mass fingerprint analysis. Some of the differentially expressed spots showed low intensities, indicating their low-abundant character. Thus it was not always possible to pick or identify spots of lowest abundance, even after pooling material from several gels.

Molecular weight and pI values of the identified proteins were checked on the 2D gel and found to be in the expected range. The significantly identified spots with fold changes and corresponding sequence coverage in percentage, MOWSE score, UniProtKB accession number (bit.ly/20VYtgg), function category and protein name are shown in Table 2.

Dose Response after Irradiation with Three Different Low Doses (IR3, IR4 and IR5)

To investigate the radiation response after three low doses differentially expressed proteins were compared between the different condition groups: IR3 (40 mGy), IR4 (100 mGy) and IR5 (140 mGy), dose rate 26,400 mGy/h.

The analysis of the raw data by PCA (Fig. 2A) for each radiation-induced condition showed that at the spot map level, groups IR3 (40 mGy) and IR4 (100 mGy) were well separated from the nonirradiated control group and that IR5 (140 mGy) differed less from the control. The three analyzed replicates formed different clusters depending on the radiation-induced conditions, revealing a stable and differentiated dose response.

To enlighten a presence of specific dose responses at the proteome level, the identified proteins were compared for the three different radiation-induced conditions (Fig. 2B). After irradiation with the highest dose (IR5: 140 mGy) only three proteins were differentially expressed as defined by the statistical borders applied. Only one of these proteins, EEF2, was in agreement with one of the other radiation-induced conditions (IR3). The levels of EEF2 observed were close to the detection limits and it cannot be excluded that the same trend was also at IR4. After 40 mGy irradiation (IR3) a total of 11 differentially expressed proteins were identified. After 100 mGy irradiation (IR4) the same number of 11 proteins, was found to be differentially expressed, but only 4 proteins were shared with IR3 (40 mGy). No single common protein could be detected that was affected at all three doses (Fig. 2B). Thus, for each dose, unique patterns of differentially expressed proteins were observed, possibly indicating that different stress-response pathways were induced.

The Effects of a Priming Dose after a Challenge Dose (IR1) Compared to a Single Challenge Dose (IR4) and to the Single Priming Dose (IR2)

For IR1 and IR4 doses we wanted to analyze whether the exposure to a priming dose given 2 h prior to a challenge dose (adaptive response) had an impact on the protein expression observed 3 h after the challenge dose. The 40 mGy priming dose was given at 50 mGy/h, while the 100 mGy challenge dose was given at the higher dose rate of 26,400 mGy/h.

Principal component analysis was performed using the raw data. The irradiated groups were well separated from the nonirradiated controls. The irradiated samples were grouped according to the applied challenge dose with (IR1) or without (IR4) the priming dose, showing that a priming dose caused a different radiation-induced response on protein level (Fig. 3A). The priming dose significantly altered the number and type of differentially regulated proteins compared to the protein expression observed when the challenge dose was given alone (IR4) (Fig. 3B).

Compared to only the priming condition (IR2), 11 of the 20 differentially expressed proteins observed 5 h postirradiation after a priming dose of 40 mGy remained differentially expressed even after an additional 100 mGy acute exposure (IR1) (Fig. 3C).

Validation of Target Proteins by Western Blotting

To validate the data obtained by 2D-DIGE, six different proteins were analyzed by Western blotting. The six selected proteins, VIM, CLIC1, LMNA, SOD, VCL and EEF2, were selected because of high statistically significant deregulation and/or availability of antibodies. In spite of the small relative changes in protein expression the regulation factors found by the 2D analysis could be verified by the Western blot analysis for the chosen examples (Table 3).

There was good agreement for all six proteins, between the relative regulation factors for DIGE 1 and DIGE 2 and for Western blot relative expression ratios. In general, it is noteworthy that under the different exposure conditions, varying doses and dose rates, the magnitude of differential protein expression is moderate for the identified proteins (Table 3) and does not exceed 187% of the corresponding control.

An example of the Western blot for VIM is shown in Fig. 4. Protein signals (Fig. 4B) were quantified and normalized to the total protein amount loaded on the corresponding lane and transferred to a nitrocellulose membrane (Fig. 4A). In the exposure conditions IR1 and IR2, vimentin expression was upregulated by a factor of 1.83 and 1.87, respectively, while a single acute dose of 140 mGy did not induce a significant change in expression (Fig. 4C).

Pathway Analysis

The largest number of subnetworks was reconstructed with IR1 (5 modules with 29 nodes) and IR2 (6 modules with 32 nodes) identifying in each case three dominant pathways, whereas IR3 (3 modules with 16 nodes) and IR4 (4 modules with 21 nodes) revealed only one major pathway (Fig. 5). With only three significantly deregulated proteins, IR5 showed no dominant pathway. IR2 (40 mGy with dose rate of 50 mGy/h) clearly had a more pronounced

TABLE 2
Differentially Regulated Proteins Identified by DeCyder Software and MALDI-TOF/TOF

Symbol	Protein name	Function category	Accession no.	MOWSE score	Sequence coverage (%)	Regulation factor				
						IR1	IR2	IR3	IR4	IR5
ALDH1A1	Aldehyde dehydrogenase family 1 member A1	Aldehyde metabolism	P00352	678	47	**1.11**	1.09	1.07	**1.14**	1.05
ALDH9A1	Aldehyde dehydrogenase family 9 member A1	Aldehyde metabolism	P49189	78	18	**1.06**	1.08	**1.07**	1.04	1.01
ACTB	Actin, beta, cytoplasmatic 1	Cellular adhesion and migration	P60709	399	60	–1.78	**–1.90**	–1.41	–1.62	–1.29
CLIC1	Chloride intracellular channel protein 1	Chloride transport, cell cycle	O00299	70	34	**1.38**	**1.50**	1.19	**1.42**	1.18
VCL	Vinculin	Cytoskeleton	P18206	354	37	1.14	**1.13**[a]	1.14	**1.20**	1.12
VCL	Vinculin	Cytoskeleton	P18206	310	40	1.05	**1.12**[a]	1.04	1.06	1.01
TUBB	Tubulin beta chain	Cytoskeleton	P07437	443	60	**1.30**	**1.18**	1.27	1.20	1.10
SEPT11	Septin 11	Cytoskeleton/ cytokinesis	D6RGI3	65	25	**1.24**	**1.29**	**1.19**	**1.22**	1.07
VIM	Vimentin	Cytoskeleton/signal transduction	P08670	246	57	**1.73**[a]	**1.53**[a]	**1.47**[a]	**1.56**	1.15
CORO1C	Coronin-1C	Cytoskeleton/signal transduction	Q9ULV4	66	16	–1.09	**1.16**	–1.04	1.08	1.05
SDHA	Succinate dehydrogenase flavoprotein subunit, mitochondrial	Energy metabolism	P31040	147	30	–1.11	–1.08	–1.09	**–1.17**	–1.05
VCP	Transitional endoplasmic reticulum ATPase	ER transport	P55072	78	20	–1.33	**–1.48**	–1.29	–1.37	–1.22
COL6A2	Collagen alpha-2(VI) chain	Extracellular matrix	P12110	129	25	**–1.35**[a]	**–1.35**[a]	–1.14	–1.17	**–1.14**
COL1A1	Collagen alpha-1(I) chain	Extracellular matrix	P02452	242	34	**–1.09**	–1.04	1.02	1.09	1.14
ACO1	Cytoplasmic aconitate hydratase	mRNA binding protein	P21399	239	34	–1.09	–1.07	–1.04	**–1.18**	–1.15
LMNA	Lamin A	Nuclear assembly	P02545	278	44	**1.21**	1.11	**1.35**[a]	**1.25**	1.0
LMNA	Lamin A	Nuclear assembly	P02545	146	39	1.24	1.20	**1.30**[a]	1.26	1.17
LMNA	Lamin A	Nuclear assembly	P02545	395	55	1.36	**1.40**	1.38	1.39	1.27
LMNB1	Lamin B1	Nuclear assembly	E9PBF6	100	38	**1.35**	1.29	1.20	1.24	1.11
SOD2	Superoxide dismutase 2 [Mn] mitochondrial	Oxidative response	P04179	283	27	**–1.44**[a]	**–1.46**[a]	–1.23	**–1.21**	–1.14
TXNRD1	Thioredoxin reductase 1. cytoplasmic	Oxidative response	E9PIR7	84	28	**1.10**	–1.01	–1.02	1.0	1.01
CCT5	T-complex protein 1 subunit epsilon	Protein folding, stress response	P48643	159	41	1.09	**1.15**	**1.18**	1.12	1.06
HSPA8	Heat shock cognate 71 kDa protein	Protein folding, stress response	P11142	120	34	**–1.19**[a]	**–1.29**[a]	**–1.27**[a]	–1.16	–1.13
CCT2	T-complex protein 1 subunit beta	Protein folding, stress response	P78371	56	18	1.07	**1.21**	1.18	1.15	1.13
HSPA5	78 kDa glucose-regulated protein	Protein folding, stress response	P11021	624	52	**–1.09**	–1.07	–1.07	–1.07	–1.06
WDR1	WD repeat-containing protein 1	Protein protein interaction	O75083	253	53	**1.11**	**1.21**	**1.14**	**1.14**	1.01
WDR1	WD repeat-containing protein 1	Protein protein interaction	O75083	181	40	**1.06**	1.11	1.08	**1.11**	1.05
EEF2	Elongation factor 2	Protein synthesis	P13639	127	20	**1.25**[a]	**1.12**	**1.19**[a]	1.03	**1.06**
EEF2	Elongation factor 2	Protein synthesis	P13639	446	46	**1.13**[a]	1.11	**1.13**[a]	1.05	**1.10**
HNRNPL	Heterogeneous nuclear ribonucleoprotein L	Protein synthesis	P14866	108	25	**1.21**	**1.27**	**1.24**	1.12	1.13

Continued on next page

TABLE 2
Continued.

Symbol	Protein name	Function category	Accession no.	MOWSE score	Sequence coverage (%)	Regulation factor				
						IR1	IR2	IR3	IR4	IR5
GARS	Glycine-tRNA ligase	Protein synthesis	P41250	227	35	1.05	1.05	1.06	1.08	**1.09**
DDX1	ATP-dependent RNA helicase DDX1	RNA helicase	Q92499	66	12	1.06	1.06	**1.08**	1.0	–1.02
ANXA6	Annexin 6	Signal transduction	P08133	344	57	**–1.10**[a]	–1.05	**–1.07**	1.01	1.02
DPYSL2	Dihydropyrimidinase-related protein 2	Signal transduction	Q16555	95	24	1.14	**1.13**	1.10	1.07	1.01
MVP	Major vault protein	Signal transduction	Q14764	183	38	1.01	**1.11**	1.11	1.06	1.12
UCHL1	Ubiquitin carboxyl-terminal hydrolase isozyme L1	Ubiquitination processes	P09936	55	28	1.13	**1.19**[a]	1.13	**1.22**	1.13
31	Number of significantly altered proteins					18	20	11	11	3

Notes. Proteins are listed according to their alphabetically ordered gene category. The statistically significant altered proteins ($P \leq 0.05$) are shown in bold-face text (control vs. treated; control = 1.0). Nonsignificant regulation factors are in plain text. A protein was identified with a MOWSE score higher than 55 (for the used version of Ensembl_human db).

[a] The fold change was also significant in the dye swap set up.

effect on the proteome compared to IR3 (40 mGy, given at a high dose rate of 26,400 mGy), as demonstrated by the larger number of differentially expressed proteins and pathways, respectively. However, due to the irradiation scheme, the difference in postirradiation incubation between IR2 and IR3 was 2 h and therefore not directly comparable.

Proteomic Analysis of Stem Cells

Differential Protein Expression Analysis of DIGE Gels

The proteome of the stem cell line ADSC in response to the exposure conditions IR1, IR4 and IR5 (Fig. 1) was also examined by employing 2D-DIGE analysis. To strengthen the statistical power, four biological replicates were analyzed. Exposure condition IR1 was chosen to investigate adaptive response effects compared to IR4. The dose-response relationship between 100 and 140 mGy acute exposure was compared for IR4 and IR5.

Statistical Evaluation of the Raw Data

For the analysis of low-dose effects in stem cells, the most interesting exposure conditions (IR1, IR4, IR5) were selected with four biological replicates to strengthen the statistical evaluation.

Between 25 and 89 regulated candidate spots (raw data) with statistically significant P values ($P \leq 0.05$) were detected by DeCyder® software, however, several of these were artefacts located at the edge of the gels and in the smear (Table 4). After visual spot confirmation only a few well separated spots could be confirmed and the fold changes on the proteome level comparing all exposure conditions were marginal compared to the results observed for VH10 cells. In the majority of cases, the corresponding regulation factors for the stem cells were in a range far below 20%.

Despite the minimum effect on the proteome the PCA analysis of the raw data revealed an interesting result, showing two main groups IR1/IR5 and IR4/control, indicating that IR4 (single 100 mGy) is similar to the nonirradiated control, whereas IR1 (priming dose 40 mGy plus challenge dose 100 mGy for total of 140 mGy) and IR5 (140 mGy) are alike (data not shown). This grouping clearly illustrates a radiation-induced effect and perhaps a threshold value. The clustering did not use any sample or replicate information.

Western Blot

We further tested if the two candidate proteins vimentin and vinculin from the VH10 experiment were also differentially expressed in ADSC. Western blot analysis delivered detectable bands for both proteins but no differential regulation for these two proteins in stem cells (data not shown).

DISCUSSION

In this study, a proteomic approach was used to analyze how the proteome in primary human fibroblasts and stem cells would change in response to low doses (40–140 mGy) and if an adaptive dose would change the protein of a challenge dose. Identifying exposure-specific protein interaction networks could be useful for the discovery of crucial radiation-linked mechanisms in the low-dose region.

Proteome Response of Human Fibroblasts (VH10) to Low Doses and Dose Rates

A comparison of the responses to different radiation doses showed that the proteome of human fibroblasts reacted moderately but characteristically according to the applied

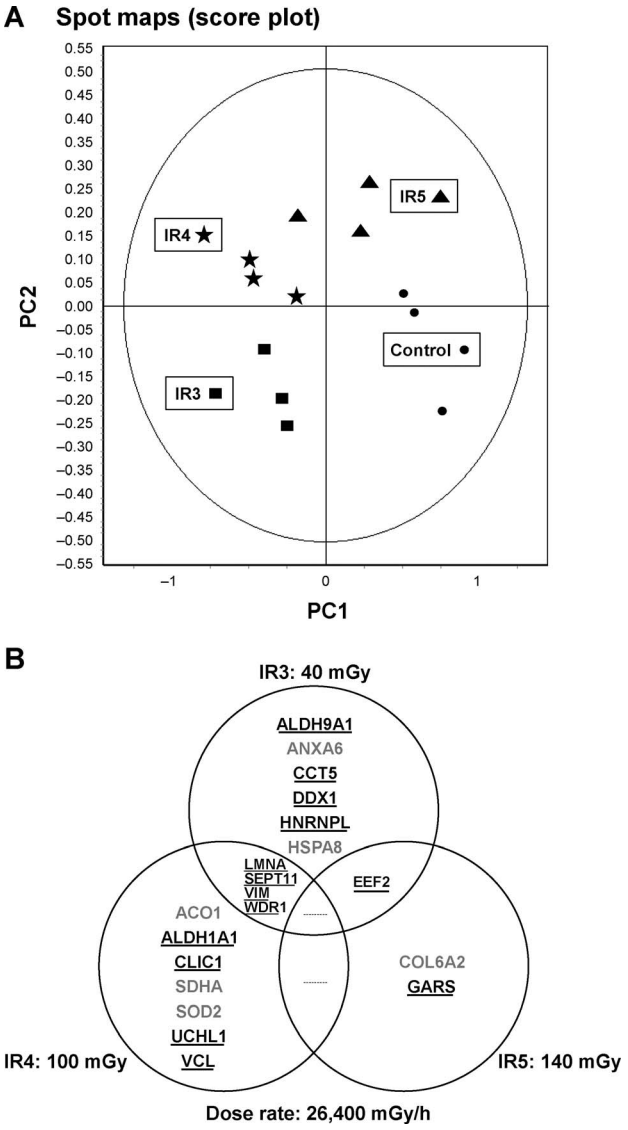

FIG. 2. Dose-response effect (dose rate 26,400 mGy/h). Panel A: Principal component analysis of the 2D-DIGE results for dose-response analysis. Protein spots found at least in 16 of 18 gel spot maps were visualized by score plot. Gels are symbol coded according to sample (IR3: rectangle; IR4: star; IR5: triangle; control: sphere). Panel B: Venn diagram of differentially regulated proteins among three different doses (40, 100 and 140 mGy). Statistically significantly deregulated proteins are shown. Up-regulated proteins are marked black and underlined, while down-regulated proteins are marked gray.

low doses. A number of significantly up- or down-regulated proteins have been described, and some candidate proteins were verified using Western blot technology. Generally, only a relatively small number of proteins were differentially expressed after irradiation, in agreement with other published studies with higher doses (*30, 31*).

Using mass spectrometry, 31 different radiation-regulated proteins could be identified. Our results show that low-dose irradiation of cells could modify signal transduction pathways, possibly orchestrating the subsequent repair mechanisms. The published literature on the effects of high-dose rates (>1 Gy/min) on the proteome is extensive and several hundred radiation-responsive proteins have been described (*32*). However, the list of differentially regulated proteins covers several of the proteins identified in this study, although doses were often larger than 4 Gy.

Basically, the identified regulated proteins could be classified into four main categories (Table 2): 1. cytoskeleton dynamics and nuclear lamin A; 2. oxidative response and damage; 3. stress response and protein processing; and 4. protein synthesis. This is an arbitrary classification, as some proteins have multiple functions and can play a role in more than one group or pathway.

Identified Proteins and Their Putative Functions in the Radiation-Induced Response Process at Low Doses

Structural Proteins

Generally, a large number of structural proteins were found to be affected. The protein with the highest regulation factor was vimentin, which was up-regulated under all radiation-induced conditions except IR5 (140 mGy). This is particularly interesting, given its pivotal role in many essential biological processes of the cell like attachment, migration and particularly cell signaling and cell cycle regulation. Vimentin has also been demonstrated to function as a potential regulator of transcription, as it is able to interact and sequester transcriptional determinants such as p53 (*33*), integrating stress-response signals e.g., after irradiation and mediating cell cycle arrest, repair and apoptosis, while it has also been shown to suppress tumor development (*34, 35*). Recent findings based on human cells exposed to space radiation suggest that p53 is involved in adaptive responses by eliciting a protective effect against low-dose radiation (*36*).

Other structural proteins affected by low-dose irradiation were lamins. The nuclear lamins and lamin-associated proteins, represent a pivotal determinant in structure and function preserving genomic stability (37), facilitating chromatin organization, DNA replication and repair, regulation of gene transcription (*38, 39*), as well as in cell cycle regulation (*40, 41*). In particular, A-type lamins are linked with a whole variety of human degenerative disorders, premature aging syndromes and cancer (*42–44*). Consistent with deficient DNA double-strand break (DSB) repair, lamins A/C-deficient cells are significantly more sensitive to radiation showing effects on cell cycle regulation as well as DNA repair (*45*). In our study, low-dose irradiation provoked expression changes of lamin A/C shown by several identified regulated isoforms with different pI values but the same molecular weight.

Another identified structural protein, membrane-cytoskeletal protein vinculin, is involved in crucial signaling cascades enabling the cells to cope with radiation-induced injuries (*46–48*) and maintaining correct cell function (*49*). Differential regulation of structural proteins namely vimen-

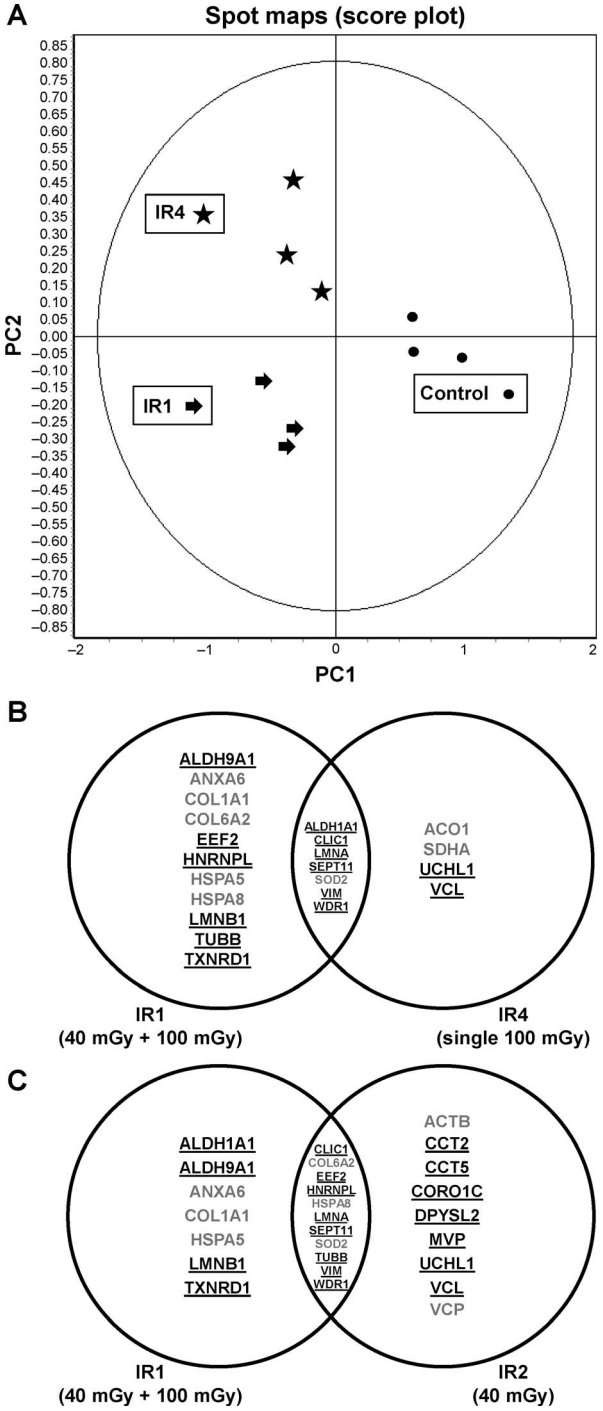

FIG. 3. Priming dose effect. Panel A: Principal component analysis for the priming dose effect. Protein spots found at least in 16 of 18 gel spot maps were visualized by score plot. Gels are symbol coded according to sample (IR1: arrow; IR4: star; control: sphere). Panel B: The Venn diagram compares the effects of a priming dose on the protein expression of a challenge dose (IR1 and IR4). Statistically significantly deregulated proteins are shown. Up-regulated proteins are marked black and underlined, while down-regulated proteins are marked gray. The differentially expressed proteins in exposure condition IR1 were compared with the single challenge dose IR4. Panel C: The Venn diagram compares the effects of a priming dose on the protein expression (IR1 and IR2). Statistically significantly deregulated proteins are shown. Upregulated proteins are marked black and underlined, while down-regulated proteins are marked gray.

tin, lamin A/C and vinculin also correlate with radiotherapy response (*50*).

Oxidative Stress-Response Proteins

We also observed the effects on key proteins involved in oxidative stress response such as SOD2 and CLIC1. The link between oxidative stress and exposure to low doses and dose rates has previously been shown in several model systems and explained to be primarily caused by an induced endogenous production of reactive oxygen species (ROS) (*3–5, 11*).

For some unknown reason SOD2 was down-regulated under the IR1 and IR2 conditions (priming dose exposure), respectively. At a low dose of 40 mGy given at a dose rate of 50 mGy/h, the cells are undergoing intense oxidative stress. This can not only lead to direct molecular damage by radicals but also influence gene expression, nuclear chromatin remodeling and posttranslational modifications of proteins (*51*) as well as long-lasting epigenetic effects (*52*). A decreased level of SOD2 also has an adverse impact on enzymes of the Krebs cycle by deploying a progressive elevation of ROS, which over time leads to a dysfunctional electron transport chain, as observed by down-regulation of succinate dehydrogenase flavoprotein subunit (SDHA), e.g., under the IR4 condition. CLIC1 was identified as being up-regulated and is a member of the chloride intracellular channel family that serves as a regulator of cell volume, pH, cell cycle and apoptosis (*53, 54*) and is regulated through redox-sensitive residues on the protein (*55, 56*). Proteomic studies identified delayed effects on the differential expression of CLIC1 in the progeny of irradiated human liver cells (*57*) or acquisition of a radioresistant phenotype by suppression of CLIC1 activity (*58*). These results suggest that CLIC1 activity is regulated by both oxidative stress and cellular relocalization triggered by radiation exposure.

Some other proteins on the candidate list, such as thioredoxin reductase 1 (TXNRD1), as well a member of the ubiquitous family of antioxidant enzymes, but also several classic heat shock proteins (HSPA8, HSPA5) support the notion that stress responses in particular are induced by low-dose exposure.

Dose Response Effects and Induced Pathways

A key goal in this study was the identification of specific pathways that might play an important role in processes modulating low-dose response. Over the past decade, it has become clear that single biomarkers, such as the expression level of a particular protein, often do not perform as well as signatures created from ensembles of proteins (*59*). Multigene signatures have been regarded as more effective

←
The differentially expressed proteins in exposure condition IR1 were compared with the single priming dose IR2.

TABLE 3
Relative Expression Changes of the Six Selected Candidate Proteins Compared to the Results of Western Blot Analysis

Protein	Total protein normalization		Control	IR1	IR2	IR5
VIM		DIGE 1	1.0	1.72[b]	1.57[a]	1.14
		DIGE 2	1.0	1.73[b]	1.53[b]	1.15
	Gel	**WB**	**1.0**	**1.83**[a]	**1.87**[b]	**1.08**
CLIC1		DIGE 1	1.0	1.27	1.46	1.11
		DIGE 2	1.0	1.38[a]	1.5[b]	1.24
	Gel	**WB**	**1.0**	**1.20**	**1.24**[a]	**1.07**
LMNA		DIGE 1	1.0		Several isoforms, all upregulated	
		DIGE 2	1.0		Several isoforms, all upregulated	
	Gel	**WB**	**1.0**	**1.53**	**1.37**	**1.64**
SOD2		DIGE 1	1.0	–1.42[b]	–1.49[b]	–1.13
		DIGE 2	1.0	–1.44[b]	–1.46[b]	–1.14
	Gel	**WB**	**1.0**	**–1.16**	**–1.21**	**–1.10**
VCL		DIGE 1	1.0	1.13	1.16[a]	1.13
		DIGE 2	1.0	1.14	1.13[a]	1.11
	Gel	**WB**	**1.0**	**1.39**[a]	**1.44**[b]	**1.46**[a]
EEF2		DIGE 1	1.0	1.28[b]	1.1	1.06[b]
		DIGE 2	1.0	1.25[b]	1.12[a]	1.02
	Gel	**WB**	**1.0**	**1.15**	**1.12**	**–1.01**

Notes. The technical replicates by dye swap are marked DIGE 1 and DIGE 2, relative expression rations are given. Western blot (WB) marked in bold-face text. Data are based on the Western blot results shown in Fig. 4 and Supplementary Fig. S1 (http://dx.doi.org/10.1667/RR14226.1.S1).

[a] $P \leq 0.05$ and [b] $P \leq 0.01$; values that are significantly different compared to the control are indicated.

than single gene expression values based on the belief that the network of gene/protein interactions produces the phenotypes displayed by cells (*60*). Identifying exposure-specific protein interaction networks could be useful for the discovery of crucial radiation linked mechanisms.

A fundamental finding in the low-dose range (40, 100 and 140 mGy) was that no linear dose-response relationship was observed regarding the relative yields of differentially up- or down-regulated proteins. The response relationships can best be described as on/off effects involving regulation of different proteins depending on dose and dose rates.

Exposure at each radiation dose resulted in a characteristic reaction pattern, while the two lower doses (40 and 100 mGy) had the most overlap (Fig. 2B). Interestingly, the highest radiation dose resulted in the lowest number of differentially expressed proteins, indicating a possible phase shift in the cellular response to doses $\geq$140 mGy. Similar observations with different dose-response patterns after low-dose radiation have been reported for the transcriptional level (*8, 61*). Overall, the number of modulated genes did not change drastically after low-dose irradiation. Clustering analysis revealed up-regulated genes related to p53 pathway and DNA damage response showing a classical dose response as well as genes with constant modulation (no change with higher doses) of their expression related to cellular respiration, ATP metabolic process and chromatin organization. Another research group (*9*) found several genes, such as cytoskeleton components and cell–cell signaling genes to respond to low-dose radiation but not to high-dose radiation which is in accordance with our results. However, DNA repair pathways were not measured directly. The unique pathway module identified under IR3 comprised a protein signature for cancer-related pathways (Fig. 5C, yellow). IR4, however, revealed mainly apoptosis related pathways (Fig. 5D, pink).

A total radiation dose of 40 mGy given with a lower dose rate (50 mGy/h) resulted in a complex interaction scheme. As shown in Fig. 5B, the IR2 condition comprised three major interaction patterns: focal adhesion and signaling processes, such as integrin (green); cell cycle regulation (blue); and a third single network cluster exhibiting several interleukin signaling pathways (orange).

TABLE 4
Number of Significantly Altered Protein Spots in ADSC Detected by Decyder Software Postirradiation

Exposure conditions	Priming dose rate (mGy/h)	Challenging dose rate (mGy/h)	Total dose (mGy)	Total spots (master gel)	Candidate spots *t* test, $P \leq 0.05$ (raw data)[a]	Confirmed spots
IR1	50	26,400	40 + 100	2,495	66	5
IR4	-	26,400	100	2,495	25	7
IR5	-	26,400	140	2,495	89	15

[a] Mean value of the four biological replicates.

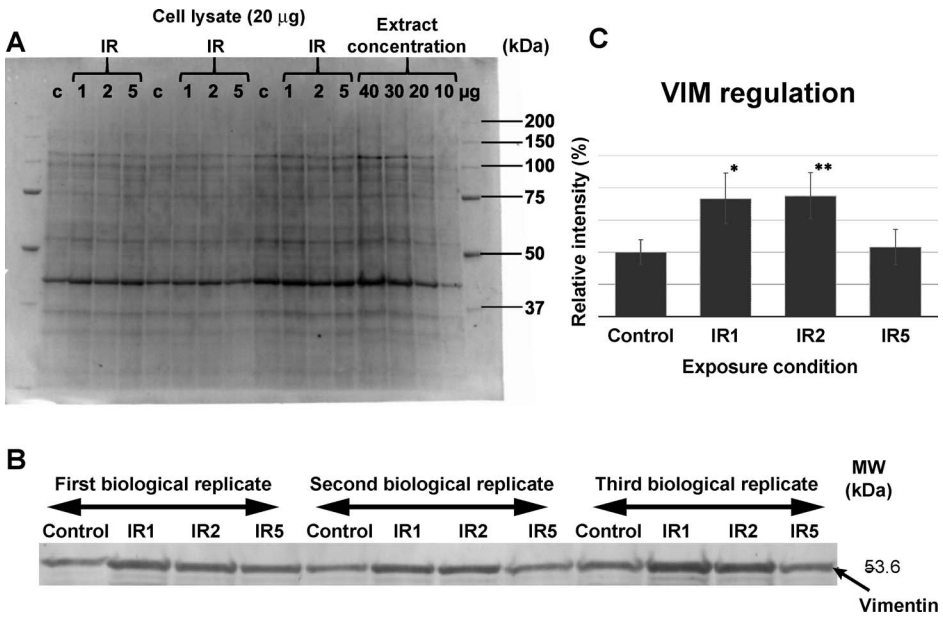

FIG. 4. Western blot results (vimentin). Panel A: Nitrocellulose membrane after protein transfer. Protein signals were quantified and normalized to the total protein amount loaded on the corresponding lane. Protein extract (20 µg) of each sample was loaded per lane (c = control; IR 1, 2, 5; extract concentration). Panel B: Original Western blot. Three biological replicates of the different exposure conditions. Panel C: Quantification of expression changes of vimentin in VH10 cells. The columns correspond to the mean values of three independent biological samples ± standard deviation. Changes relative to the control set as 100% are shown. The asterisks denote values that are significantly different from control, *P = 0.05, **P = 0.01. The up-regulation verified by Western blot confirmed the regulation factors which were obtained by the 2D-DIGE approach (see Table 3).

Effects of a Priming Dose and Triggered Pathways

Based on the adaptive response conditions (IR1) performed with a priming dose of 40 mGy at a low dose rate (50 mGy/h) followed by a challenge dose of 100 mGy (26,400 mGy/h) and the corresponding controls, several interesting results were observed. A priming dose significantly altered the radiation response of the challenge dose (Tables 1 and 2) and resulted in a more intense regulation on the protein level than the single challenge dose of 100 mGy (IR4) alone, as demonstrated by higher regulation factors of differentially regulated proteins and an increased number of differentially regulated proteins (11 to 18 proteins; Table 2). Seven of these proteins were observed under both conditions. These results suggest that the response pathways triggered by a 100 mGy challenge dose were significantly modified by the priming dose. The priming dose alone (IR2) and the combined exposure (IR1) had a similar impact on the proteome response. Also, when the 100 mGy dose (IR4) was compared with IR1 the dominating effect of the priming dose was evident. In fact, IR1 and IR2 appear to be much more similar to each other than IR1 and IR4. This might lead to the hypothesis that the pathways induced by the priming dose are predominant and may reflect basic pathways for cellular stress response.

As shown in Fig. 5A, the three most prominent pathways for IR1 were linked to focal adhesion and signaling processes, e.g., integrin (blue) and to cell cycle regulation (green). The third relevant module under IR1 mainly displays the pathways that are involved in apoptosis (pink). Interestingly, a cell death-related network was significant only in response to radiation condition IR4. Exposure to the priming dose (IR1, IR2) resulted in the most complex interaction network, in agreement with the finding that 40 mGy delivered at 50 mGy/h had the greatest effect on the proteome of the cells.

Proteome Response of Human ADSC to Low Doses and Dose Rates

In marked contrast to the research on the effects of radiation on various types of somatic cells, studies on the response of human stem cells to low doses of radiation are rare. Stem cell differentiation is a major factor with implications in the radiosensitivity of a given tissue, and the radiobiology of cancer stem cells is a focus of clinical applications. Hence, stem cell sensitivity may be essential for the overall sensitivity of a biological system. In this study, the effects of low doses and dose rates on the proteome of the ADSC followed the irradiation protocol developed for the cell cultures of the human VH10 fibroblasts for direct comparison. As stem cells inherently possess several distinct characteristics that set them apart from other cell types, their responses to radiation may be completely different compared to fibroblast cells. The intriguing results, shown in Table 4, suggest that the proteome of ADSC differ significantly compared to the human fibroblasts in response to low doses of radiation (IR1, IR4 and IR5). The number of differentially

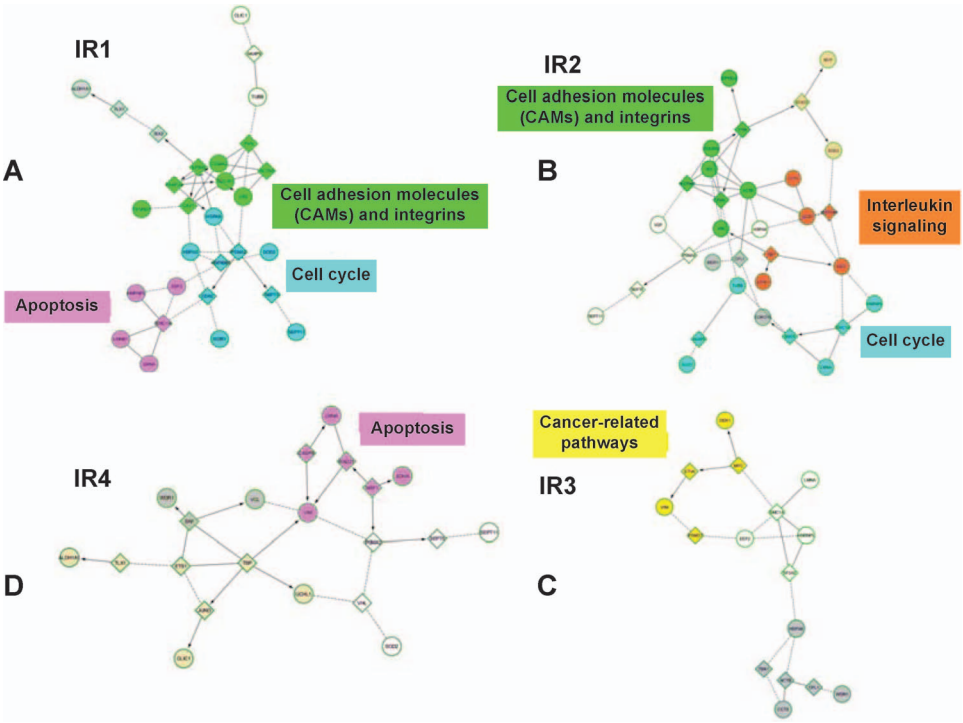

FIG. 5. Reactome FI functional interaction network in response to different irradiation conditions. Panel A: For IR1 the network is reconstructed of 29 nodes, divided in 5 subclusters (modules). Sixteen of eighteen proteins from the list are present in the network. Thirteen linker proteins were added to complete the network. The nodes are cross-linked through 43 edges. The modules are color coded corresponding to the most dominant pathways [blue = regulation of cell cycle, pink = regulation of apoptosis, green = cell adhesion molecules (CAMs) and integrin signaling]. Modules without significant network are indicated in gray and white. Panel B: The network for IR2 is built up of 32 nodes, which are subclustered in 6 modules. Twenty proteins from the list are existent in the network. Twelve linker proteins were added to reconstruct the network. The nodes are cross-linked through 51 edges. The modules are color coded corresponding to the most dominant pathways [blue = regulation of cell cycle, green = cell adhesion molecules (CAMs) and integrin signaling and orange = interleukin signaling]. Modules without significant network are indicated in gray, white and cream. Panel C: The IR3 network contains 16 nodes, subclustered in 3 modules. Eight of eleven proteins from the list are existent in the network. Eight linker proteins were added to build the network. Nineteen edges cross-link the nodes. Modules are color coded corresponding to the most dominant pathways (yellow = cancer related pathways). Modules without significant network are indicated in gray and white. Panel D: The IR4 network comprises 21 nodes, subclustered in 4 modules. Ten of eleven proteins from the list are integrated in the network. Eleven linker proteins were added to reconstruct the network. The nodes are cross-linked through 26 edges. The modules are color coded corresponding to the most dominant pathways (pink = regulation of apoptosis). Modules without significant network are indicated in gray, white and cream.

up- or down-regulated proteins were markedly reduced compared to VH10 cells indicating that the ADSC stress-response pathways have a different stress-response threshold. In a recently published review, different human stem cells (hSCs) were examined for their specific responses to radiation (*62*). Human embryonic stem cells (hESCs) and adult hSCs that populate corresponding tissues, such as human mesenchymal stem cells (hMSCs), human hematopoietic stem cells (hHSCs), neural and intestinal hSCs, etc., clearly show unique characteristics in radiation-induced response. hESCs were observed to undergo apoptosis at doses exceeding the low-dose range and hHSCs were found to be exquisitely sensitive to radiation, responding with massive apoptosis to even modest doses of radiation (>1 Gy). Intriguingly, human mesenchymal stem cells were observed to be relatively resistant to low-dose exposures and since adipose tissue is derived from the mesenchyme and represents the source of ADSC, this could explain their robustness.

The preliminary results for ADSC presented here prompt the need for more thorough studies over a wider dose range and dose rates, to better characterize the possible differences in the regulation of the proteome compared to differentiated cells.

CONCLUSION

The proteome of human fibroblasts in culture undergoes unique changes in response to small changes in radiation dose. For the investigated dose range (40–140 mGy) no linear dose-response relationships were observed regarding the relative yields of differentially up- or down-regulated proteins. The response relationships can best be described as on/off effects involving different proteins depending on dose and dose rate.

A priming dose significantly altered the proteome regulation by a challenge dose, i.e., the protein response pathways triggered by 100 mGy acute gamma radiation was

significantly modified when a priming dose was given. Although these results are still preliminary, this interesting finding may in part depend on the low-dose rate used for the priming dose (50 mGy/h), as the priming most efficiently induced differentially regulated pathways (see summary in Supplementary Table S1; http://dx.doi.org/10.1667/RR14226.1.S1).

The proteome of ADSC differed significantly compared to the VH10 human fibroblast in response to low doses of radiation. The number of differentially up- or down-regulated proteins were markedly reduced compared to VH10 cells, indicating that the ADSC stress-response pathways have a different threshold. Primarily, the structural and stress-response proteins were affected, leading to different signaling and repair pathways.

Further investigation is needed to gain a better understanding of the mechanisms initiated by low doses of ionizing radiation. The results from this work support the idea that studies of the proteome can provide new insights into the cellular responses to low doses of ionizing radiation, thus enabling a better understanding and subsequently, adequate risk estimations in the future.

SUPPLEMENTARY INFORMATION

Table S1. Summary of key findings (VH10 fibroblasts).

Figure S1. Western blots of candidate proteins and quantification of expression changes.

ACKNOWLEDGMENTS

This project was performed with financial support from the European DoReMi Program (Low Dose Research towards Multidisciplinary Integration, grant no. EC 249689). The work at Stockholm University was also supported by the Swedish Radiation Safety Authority. Work performed by AD was supported by the German Federal Ministry of Education and Research, grant no. 02NUK24A. The authors declare no conflict of interest.

Received: August 11, 2015; accepted: January 14, 2016; published online: 00 00, 00

REFERENCES

1. The 2007 Recommendations of the International Commission on Radiological Protection. ICRP publication 103. Ann ICRP 2007; 37:1–332.
2. Mullenders L, Atkinson M, Paretzke H, Sabatier L, Bouffler S. Assessing cancer risks of low-dose radiation. Nat Rev Cancer 2009; 9:596–604.
3. Haghdoost S, Czene S, Naslund I, Skog S, Harms-Ringdahl M. Extracellular 8-oxo-dG as a sensitive parameter for oxidative stress in vivo and in vitro. Free Radic Res 2005; 39:153–62.
4. Haghdoost S, Sjolander L, Czene S, Harms-Ringdahl M. The nucleotide pool is a significant target for oxidative stress. Free Radic Biol Med 2006; 41:620–6.
5. Sangsuwan T, Haghdoost S. The nucleotide pool, a target for low-dose gamma-ray-induced oxidative stress. Radiat Res 2008; 170:776–83.
6. Bajinskis A, Lindegren H, Johansson L, Harms-Ringdahl M, Forsby A. Low-dose/dose-rate gamma radiation depresses neural differentiation and alters protein expression profiles in neuroblastoma SH-SY5Y cells and C17.2 neural stem cells. Radiat Res 2011; 175:185–92.
7. Skiöld S, Azimzadeh O, Merl-Pham J, Naslund I, Wersall P, Lidbrink E, et al. Unique proteomic signature for radiation sensitive patients: a comparative study between normo-sensitive and radiation sensitive cancer patients. Mutat Res/Fundam Mol Mech Mutagen 2015; 776:128–35.
8. Amundson SA, Lee RA, Koch-Paiz CA, Bittner ML, Meltzer P, Trent JM, et al. Differential responses of stress genes to low dose-rate gamma irradiation. Mol Cancer Res 2003; 1:445–52.
9. Ding LH, Shingyoji M, Chen F, Hwang JJ, Burma S, Lee C, et al. Gene expression profiles of normal human fibroblasts after exposure to ionizing radiation: a comparative study of low and high doses. Radiat Res 2005; 164:17–26.
10. Franco N, Lamartine J, Frouin V, Le Minter P, Petat C, Leplat JJ, et al. Low-dose exposure to gamma rays induces specific gene regulations in normal human keratinocytes. Radiat Res 2005; 163:623–35.
11. Yentrapalli R, Azimzadeh O, Sriharshan A, Malinowsky K, Merl J, Wojcik A, et al. The PI3K/Akt/mTOR pathway is implicated in the premature senescence of primary human endothelial cells exposed to chronic radiation. PLoS One 2013; 8:e70024.
12. Yang F, Stenoien DL, Strittmatter EF, Wang J, Ding L, Lipton MS, et al. Phosphoproteome profiling of human skin fibroblast cells in response to low- and high-dose irradiation. J Proteome Res 2006; 5:1252–60.
13. Hei TK, Zhou H, Ivanov VN, Hong M, Lieberman HB, Brenner DJ, et al. Mechanism of radiation-induced bystander effects: a unifying model. J Pharm Pharmacol 2008; 60:943–50.
14. de Toledo SM, Asaad N, Venkatachalam P, Li L, Howell RW, Spitz DR, et al. Adaptive responses to low-dose/low-dose-rate gamma rays in normal human fibroblasts: the role of growth architecture and oxidative metabolism. Radiat Res 2006; 166:849–57.
15. Morgan WF. Will radiation-induced bystander effects or adaptive responses impact on the shape of the dose response relationships at low doses of ionizing radiation? Dose Response 2006; 4:257–62.
16. Olivieri G, Bodycote J, Wolff S. Adaptive response of human lymphocytes to low concentrations of radioactive thymidine. Science 1984; 223:594–7.
17. Shadley JD, Wiencke JK. Induction of the adaptive response by X-rays is dependent on radiation intensity. Int J Radiat Biol 1989; 56:107–18.
18. Ojima M, Eto H, Ban N, Kai M. Radiation-induced bystander effects induce radioadaptive response by low-dose radiation. Radiat Prot Dosimetry 2011; 146:276–9.
19. Wakeford R, Tawn EJ. The meaning of low dose and low dose-rate. J Radiol Prot 2010; 30:1–3.
20. Elmore E, Lao XY, Kapadia R, Giedzinski E, Limoli C, Redpath JL. Low doses of very low-dose-rate low-LET radiation suppress radiation-induced neoplastic transformation in vitro and induce an adaptive response. Radiat Res 2008; 169:311–8.
21. Amundson SA, Chen DJ. Inverse dose-rate effect for mutation induction by gamma-rays in human lymphoblasts. Int J Radiat Biol 1996; 69:555–63.
22. Vilenchik MM, Knudson AG, Jr. Inverse radiation dose-rate effects on somatic and germ-line mutations and DNA damage rates. Proc Natl Acad Sci U S A 2000; 97:5381–6.
23. Manesh SS, Deperas-Kaminska M, Fotouhi A, Sangsuwan T, Harms-Ringdahl M, Wojcik A, et al. Mutations and chromosomal aberrations in hMTH1-transfected and non-transfected TK6 cells after exposure to low dose rates of gamma radiation. Radiat Environ Biophys 53:417–25.
24. Unlu M, Morgan ME, Minden JS. Difference gel electrophoresis: a

single gel method for detecting changes in protein extracts. Electrophoresis 1997; 18:2071–7.

25. Alban A, David SO, Bjorkesten L, Andersson C, Sloge E, Lewis S, et al. A novel experimental design for comparative two-dimensional gel analysis: two-dimensional difference gel electrophoresis incorporating a pooled internal standard. Proteomics 2003; 3:36–44.
26. Sarioglu H, Brandner S, Jacobsen C, Meindl T, Schmidt A, Kellermann J, et al. Quantitative analysis of 2,3,7,8-tetrachlorodibenzo-p-dioxin-induced proteome alterations in 5L rat hepatoma cells using isotope-coded protein labels. Proteomics 2006; 6:2407–21.
27. Gurtler A, Kunz N, Gomolka M, Hornhardt S, Friedl AA, McDonald K, et al. Stain-free technology as a normalization tool in Western blot analysis. Anal Biochem 2013; 433:105–11.
28. Ladner CL, Yang J, Turner RJ, Edwards RA. Visible fluorescent detection of proteins in polyacrylamide gels without staining. Anal Biochem 2004; 326:13–20.
29. Cline MS, Smoot M, Cerami E, Kuchinsky A, Landys N, Workman C, et al. Integration of biological networks and gene expression data using Cytoscape. Nat Protoc 2007; 2:2366–82.
30. Kedracka-Krok S, Jankowska U, Elas M, Sowa U, Swakon J, Cierniak A, et al. Proteomic analysis of proton beam irradiated human melanoma cells. PLoS One 2014; 9:e84621.
31. Gurtler A, Hauptmann M, Pautz S, Kulka U, Friedl AA, Lehr S, et al. The inter-individual variability outperforms the intra-individual variability of differentially expressed proteins prior and post irradiation in lymphoblastoid cell lines. Arch Physiol Biochem 2014; 120:198–207.
32. Marchetti F, Coleman MA, Jones IM, Wyrobek AJ. Candidate protein biodosimeters of human exposure to ionizing radiation. Int J Radiat Biol 2006; 82:605–39.
33. Ivaska J, Pallari HM, Nevo J, Eriksson JE. Novel functions of vimentin in cell adhesion, migration, and signaling. Exp Cell Res 2007; 313:2050–62.
34. Woods DB, Vousden KH. Regulation of p53 function. Exp Cell Res 2001; 264:56–66.
35. Efeyan A, Serrano M. p53: guardian of the genome and policeman of the oncogenes. Cell Cycle 2007; 6:1006–10.
36. Takahashi A, Su X, Suzuki H, Omori K, Seki M, Hashizume T, et al. p53-dependent adaptive responses in human cells exposed to space radiations. Int J Radiat Oncol Biol Phys 2010; 78:1171–6.
37. Gonzalez-Suarez I, Gonzalo S. Nurturing the genome: A-type lamins preserve genomic stability. Nucleus 2010; 1:129–35.
38. Dittmer TA, Misteli T. The lamin protein family. Genome Biol 2011; 12:222.
39. Andres V, Gonzalez JM. Role of A-type lamins in signaling, transcription, and chromatin organization. J Cell Biol 2009; 187:945–57.
40. Manju K, Muralikrishna B, Parnaik VK. Expression of disease-causing lamin A mutants impairs the formation of DNA repair foci. J Cell Sci 2006; 119:2704–14.
41. Gonzalez-Suarez I, Redwood AB, Perkins SM, Vermolen B, Lichtensztejin D, Grotsky DA, et al. Novel roles for A-type lamins in telomere biology and the DNA damage response pathway. EMBO J 2009; 28:2414–27.
42. Willis ND, Wilson RG, Hutchison CJ. Lamin A: a putative colonic epithelial stem cell biomarker which identifies colorectal tumours with a more aggressive phenotype. Biochem Soc Trans 2008; 36:1350–3.
43. Worman HJ, Ostlund C, Wang Y. Diseases of the nuclear envelope. Cold Spring Harb Perspect Biol 2010; 2:a000760.
44. Ho CY, Lammerding J. Lamins at a glance. J Cell Sci 2012; 125:2087–93.
45. Redwood AB, Gonzalez-Suarez I, Gonzalo S. Regulating the levels of key factors in cell cycle and DNA repair: new pathways revealed by lamins. Cell Cycle 2011; 10:3652–7.
46. Carisey A, Ballestrem C. Vinculin, an adapter protein in control of cell adhesion signalling. Eur J Cell Biol 2011; 90:157–63.
47. Subauste MC, Pertz O, Adamson ED, Turner CE, Junger S, Hahn KM. Vinculin modulation of paxillin-FAK interactions regulates ERK to control survival and motility. J Cell Biol 2004; 165:371–81.
48. Zemljic-Harpf AE, Godoy JC, Platoshyn O, Asfaw EK, Busija AR, Domenighetti AA, et al. Vinculin directly binds zonula occludens-1 and is essential for stabilizing connexin-43-containing gap junctions in cardiac myocytes. J Cell Sci 127:1104–16.
49. Wang Y, Kuramitsu Y, Ueno T, Suzuki N, Yoshino S, Iizuka N, et al. Proteomic differential display identifies upregulated vinculin as a possible biomarker of pancreatic cancer. Oncol Rep 2012; 28:1845–50.
50. Smith L, Qutob O, Watson MB, Beavis AW, Potts D, Welham KJ, et al. Proteomic identification of putative biomarkers of radiotherapy resistance: a possible role for the 26S proteasome? Neoplasia 2009; 11:1194–207.
51. Miriyala S, Holley AK, St Clair DK. Mitochondrial superoxide dismutase–signals of distinction. Anticancer Agents Med Chem 2011; 11:181–90.
52. Cyr AR, Hitchler MJ, Domann FE. Regulation of SOD2 in cancer by histone modifications and CpG methylation: closing the loop between redox biology and epigenetics. Antioxid Redox Signal 2013; 18:1946–55.
53. Jentsch TJ, Stein V, Weinreich F, Zdebik AA. Molecular structure and physiological function of chloride channels. Physiol Rev 2002; 82:503–68.
54. Ulmasov B, Bruno J, Woost PG, Edwards JC. Tissue and subcellular distribution of CLIC1. BMC Cell Biol 2007; 8:8.
55. Singh H, Ashley RH. Redox regulation of CLIC1 by cysteine residues associated with the putative channel pore. Biophys J 2006; 90:1628–38.
56. Littler DR, Harrop SJ, Fairlie WD, Brown LJ, Pankhurst GJ, Pankhurst S, et al. The intracellular chloride ion channel protein CLIC1 undergoes a redox-controlled structural transition. J Biol Chem 2004; 279:9298–305.
57. Zuo YH, Wang XL, Li JG, Dang XH, Wang ZW, Zhang SP, et al. Proteomic alterations in progeny of irradiated human liver cells. J Toxicol Environ Health A 2010; 73:520–8.
58. Kim JS, Chang JW, Yun HS, Yang KM, Hong EH, Kim DH, et al. Chloride intracellular channel 1 identified using proteomic analysis plays an important role in the radiosensitivity of HEp-2 cells via reactive oxygen species production. Proteomics 2010; 10:2589–604.
59. Hartwell L, Mankoff D, Paulovich A, Ramsey S, Swisher E. Cancer biomarkers: a systems approach. Nat Biotechnol 2006; 24:905–8.
60. Vidal M, Cusick ME, Barabasi AL. Interactome networks and human disease. Cell 2011; 144:986–98.
61. Nosel I, Vaurijoux A, Barquinero JF, Gruel G. Characterization of gene expression profiles at low and very low doses of ionizing radiation. DNA Repair (Amst) 2013; 12:508–17.
62. Sokolov M, Neumann R. Lessons learned about human stem cell responses to ionizing radiation exposures: a long road still ahead of us. Int J Mol Sci 2013; 14:15695–723.